行政院國家科學委員會補助專題研究計畫成果報告

※※※※※※※※※※※※※※※※※※※※※※※※※※
※　　　　　　　　　　　　　　　　　　　　　　　　※
※　三元 Si-C-N 材料場效發射顯示技術之研究(III)　※
※　　　　　　　　　　　　　　　　　　　　　　　　※
※　　　　　　　　　　　　　　　　　　　　　　　　※
※※※※※※※※※※※※※※※※※※※※※※※※※※

計畫類別：■個別型計畫　□整合型計畫
計畫編號：NSC 90－2216－E－009－034－
執行期間： 90 年 8 月 1 日至 90 年 7 月 31 日

計畫主持人：郭正次
共同主持人：
計畫參與人員：張惠林，林兆焄，汪俊翰

本成果報告包括以下應繳交之附件：
□赴國外出差或研習心得報告一份
□赴大陸地區出差或研習心得報告一份
□出席國際學術會議心得報告及發表之論文各一份
□國際合作研究計畫國外研究報告書一份

執行單位：國立交通大學材料科學與工程研究所

中　華　民　國 91 年　　月　　日

行政院國家科學委員會專題研究計畫成果報告

三元 Si-C-N 材料場效發射顯示技術之研究(III)

Forming Si-C-N crystals and Si-C-N nanotubes by microwave plasma enhanced chemical vapor deposition

計畫編號：NSC 90-2216-E-009-034
執行期限：90 年 8 月 31 日至 91 年 7 月 31 日
主持人：郭正次　國立交通大學材料科學系
計畫參與人員：張惠林，林兆君，汪俊翰

一、Abstract

Catalyst-assisted Si-C-N nanotubes and Si-C-N crystals were synthesized by gaseous sources of $CH_4/N_2/H_2$ and CH_4/N_2, respectively, and using solid Si columns symmetrically around the specimen as additional Si sources. The formation of the tubular structure is related to the ambient of process including H_2 gas. The H_2 gas is considered to delay the action of the so-called catalyst poisons and keep open the tube end for growth. SEM results show that the Si-C-N crystals are tetragonal or hexagonal shapes, a micron in size. Also, the Si-C-N tubes are random orientated with various tube diameters. The microstructures and bonding structures of Si-C-N crystals and Si-C-N tubes are investigated using TEM, XPS, and EELS.
關鍵詞：Nanotube、Crystals、Catalyst

二、Experiment

Si-C-N crystals and Si-C-N nanotubes were synthesized on Co (100 nm) coated Si wafers using a microwave plasma chemical vapor deposition (MPCVD) system, where Co film was formed by physical vapor deposition (PVD). The additional Si sources were inserted into specimen holder symmetrically around the specimen. Figure 1 schematically shows process conditions and the positions of Si columns relative to the sample. The synthesis steps were as follows. (1) H_2 reduction for 10 min at 5 Torr, and a microwave power of 500 W, followed by (2) introduction of CH_4/N_2 or $CH_4/N_2/H_2$ process gases, in a ratio of 10/100 sccm or 10/100/50 sccm, at a deposition pressure of 12 Torr, respectively, and a microwave power of 800 W, for four hours. SEM was employed to examine the film morphologies. The Si-C-N film compositions and bonding structures were determined by XPS (Microteck MT-500). TEM (Philips Techni 20) was used to characterize microstructures of the nanotubes, and electron energy loss spectroscopy (EELS) equipped with TEM was used to determine the bonding structures of NTs.

三、Results and discussion

Si-C-N crystals and Si-C-N nanotubes were synthesized with the same process parameters except the gaseous source of the former was a mixtures of CH_4/N_2 gases and that of the later was at $CH_4/N_2/H_2$ gases. Figure 2(a) shows the typical Si-C-N crystal morphologies, which are similar to those in our previous work,[2-4] in which tetragonal or hexagonal facet crystals of μm size were observed. Meanwhile, Fig. 2 (b) shows the tubular-like structures of Si-C-N indicating the random orientations and various tube diameters. The effect of the H_2 gas on either the Si-C-N crystal or the Si-C-N tube formations is interesting and can be interpreted in the following two ways. The first is that hydrogen removes the graphite overlayer coated on the surface of catalyst particle. This overlayer hinders the carbon atoms' desorbing and dissolving in the catalyst particles, equivalent to blocking the catalytic action of the transition metal.[25] Accordingly, the "clean" surface exposed by H_2 etching allows the succeeding C atoms to

dissolve in the catalyst, and then to precipitate a graphite-like structure around the catalyst particle. Tubular like structures are thus formed. The second interpretation is that H_2 gas promotes the graphite-like structure formation. Reconstruction of the end of the tube by H_2 atoms can prolong the tube "opening",[26] since the H_2 atoms bond to the exposed dangling bonds of carbon. Here, the role of the catalyst in forming Si-C-N tubes is similar to that of the proposed models of Baker et al.[27], Oberlin et al.[28] and Tibbetts,[29] who employed the concepts of the vapor-liquid-solid model.[30] The tube grows by precipitation of graphite sheets from a super-saturated catalytic droplet. The formation of curved graphite basal plane is energetically favorable, and so the tubular structure is formed. The base growth model is suggested to dominate the growth of Si-C-N nanotubes because the catalyst particle at the tip of the tube was not observed in the SEM top view investigation. In comparison, the catalytic functions of the process ambient without H_2 gas differ from with H_2 gas. The catalysts are suggested to provide nucleation sites for Si-C-N crystal nucleation, and effectively reduce the energy of formation at initial stage. As the growing film covers the catalytic particle, the catalytic function is lost. The film morphologies depend on the buffer layer and substrate treatment according to our previous study,[2] because the extra buffer layer, such as Fe or Co, can markedly increase the film deposition rate, which result is proven by the higher deposition rate when a catalyst is added (2.5 μm/hr) than that none is added (1 μm/hr). Figure 3 schematically shows the growth mechanisms of Si-C-N crystals and Si-C-N nanotubes. The Si-C-N crystals are formed in the process ambient without H_2 gas, while the Si-C-N nanotubes are formed in the process ambient with H_2 gas.

The XPS and EELS were selected, to identify the bonding structure of Si-C-N crystal and Si-C-N nanotube, respectively. Figure 4 shows high resolution XPS scans of core levels of Si (2p), C(1s) and N(1s). These spectra deconvoluted by Gaussian fitting consist of sub-peaks. The deconvolved peaks shows that the bonding of Si(2p)-Si, Si(2p)-N, C(1s)-C, C(1s)-N, C(1s)=N, N(1s)-Si, N(1s)-C and N(1s)=C are at 99.8 eV, 103.4 eV, 284.5 eV, 286.7 eV, 288.7 eV, 397.7 eV, 399.1 eV and 400.4 eV, respectively. In conclusion, the Si-C-N crystals are multi-bonding structures. Figure. 5 shows the EELS spectrum of Si-C-N nanotubes and the corresponding HRTEM image. The K-shell ionizations of C, N and Si occur at 288 eV, 401 eV and 1838 eV, respectively. For carbon K edge, the fine defined structure of the π^* and σ^* pre-ionization edges are characteristics of sp^2 hybridization of graphite structure. Nevertheless, the carbon K edge in these results deviates from ideal sp^2 hybridization, since the π^* fine feature (288 eV, as the indicated by the arrow) shifts to the higher energy as compared with that of graphite (284 eV). The σ^* peak at 299 eV, however, is clearly shown. For nitrogen K edge, the observed π^* transition and σ^* feature correspond to the sp^2 hybridization. The observed 401 eV π^* peak is consistent with the energy of the predicted peak (401~403 eV) that corresponds to replaced carbon by the trivalent nitrogen in a hexagonal lattice,[31] revealing the bonding structure of N atoms in an Si-C-N nanotube network. Notably, the spilt of the σ^* fine feature in nitrogen K edge is also observed. Some researchers consider that the split or round shape of σ^* peak is related to the presence of pentagonal defects and corrugations with sp^3-bonding character.[32, 33] Here, both the shift of carbon π^* edge and the split of the nitrogen σ^* edge are considered to be related to the presence of additional Si atoms in tube structures. The introducing of N and Si atoms into the carbon nanotube structure may cause distortion; change the bonding in pentagonal, heptagonal or other crystal lattices, and promote bending stress. The tube structures are thus distorted by forming bamboo-like structures, and the stress may determine the compartment size of the bamboo structure. Figures. 6(a) and 6(b) shows the TEM and HRTEM images of Si-C-N nanotubes. The inset zoom-in image shows the locally graphite-like structure. Interestingly, the

spacing between two layers is 0.35~0.37 nm larger than that of pure CNT, 0.34 nm. Si addition in Si-C-N nanotubes is worthy of study.

四、Conclusions

In conclusion, catalyst-assisted Si-C-N crystals and Si-C-N nanotubes were synthesized without and with introducing H_2 gas into the precursor gaseous source. The H_2 gas removes the C overlayer on catalyst particles, to allow succeeding C atoms to dissolve in the catalyst, since this coated film on catalyst surface hinders the catalytic action. Also, the reconstruction of tube end by H atoms that decorate the exposed C dangling bond can prolong the tube "opening" for the tube growth. The XPS results show that Si-C-N crystals consist of multi-bonding structures. Adding Si atoms in the C-N network is believed to be an interesting subject for further study. The unique differences between the nanotubes and the bulk films have opened up many scientific and technological possibilities.

五、References

1 A. Y. Liu and M. L. Cohen, Science 245, 841(1989).
2 H. L. Chang and C. T. Kuo, Diam .Relat. Mat. 10, 1910 (2001).
3 H. L. Chang and C. T. Kuo, Jpn. J. Appl. Phys. 40, 7018 (2001).
4 H. L. Chang and C. T. Kuo, Mat. Chem. Phys. 72, 236 (2001).
5 S. Muhl and J. M. Méndez, Diam. Relat. Mat. 8, 1809 (1999).
6 L. C. Chen, C. T. Wu, J. J. Wu, K. H. Chen, Inten. J. Mod. Phys. B14, 333 (2000).
7 A. Badzian, T. Badzian, R. Roy and W. Drawl, Thin Solid Films 355/356, 417 (1999).
8 L.C. Chen, C. K. Chen, S. L. Wei, D. M. Bhusari, K. H. Chen, Y. F. Chen, Y. C. Jong and Y. S. Huang, Appl. Phys. Lett. 72, 2463 (1998).
9 M. S. Wong and W. D. Sproul, J. Appl. Phys. 74, 219 (1993).
10 H. W. Kroto, J. R. Health, S. C. Óbrien, R. F. Curl and R. E. Smally, Nature 318, 162 (1985).
11 S. Iijima, Nature 354, 56 (1991).
12 R. C. Haddon, A. F. Hebard, M. J. Posseinsky, D. W. Murhy, S. J. Duclos, K. B. Lyons, B. Miller, J. M. Rosamilia, R. M. Fleming, A. R. Kortan, S. H. Glarum, A. V. Makhija A. J. Muller, R. H. Eick, S. M. Zahurak, R. Tycko, G. Dabbagh and F. A. Thiel, Nature 350, 320 (1991).
13 H. Dai, J. H. Hafner, A. G. Rinzler, D. T. Rinzler, D. T. Colbert, R. E. Smalley, Nature 384, 147 (1996).
14 G. Che, B. B. Lakshmi, E. R. Fisher, C. R. Martin, Nature 393, 346 (1998).
15 C. Journet, W. K. Maser, P. Bernier, A. Loiseau, M. Lamy de la Chapelle, S. Lefrant, P. Deniered, R. Lee and J. E. Ficher, Nature 308, 756 (1997).
16 A. C. Dillon, K. M. Jones, T. A. Bekkedahl, C. H. Kiang, D. S. Bethune and M. J. Heben, Nature 386, 377 (1997).
17 F. Ito, K. Konuma and A. Okamoto, J. Appl. Phys. 89, 8141 (2001).
18 Q. H. Wang, A. A. Setlur, J. M. Lauerhaas, J. Y. Dai, E. W. Seelig and R. P. H. Chang, Appl Phys. Lett. 72, 22 (1998).
19 R. Tenne, L. Margulis, M. Genut and G. Hodes, Nature 360, 444 (1992).
20 M. Remskar, Z. Skraba, F. Cleton, R. Sanjines and F. Levy, Appl. Phys. Lett. 69, 351 (1996).
21 N. G. Chopra, R. J. Luyken, K. Cherrey. V. H. Gespi, M. L. Cohen, S. G. Loute, A. Zettl, Science 269, 966 (1995).
22 P. M. Ajayan, O. Stephan, P. Reslich, C. Colliex, Nature 375, 564 (1995).
23 E. G. Wang, Adv. Mater. 11, 1129 (1999).
24 J. L. Zimmerman, R. Williams, V. N. Khabashesku and J. L. Margrave, Nano Lett. 1, 731 (2001).
25 M. S. Kim, N. M. Rodriguez and R.T. K. Baker, J. Catalysis 131, 60 (1991).
26 M. S. Dresslhaus, G. Dresslhaus, P. Avouris, Carbon Nanotube, Springer Press: New York, 2001; p. 65.
27 R. T. K. Baker, M. A. Barber, P. S. Harris, F. S. Feates, R. J. Waite, J. Catalysis 26, 51 (1972).
28 A. Oberlin, M. Endo, T. Koyama, J. Crystl. Growth 32, 335 (1976).
29 G. G. Tibbetts, J. Crystl. Growth 66, 632 (1984).
30 R. S. Wagner, W. C. Ellis, Appl. Phys. Lett. 4, 89 (1964).
31 J. Casanovas, J. M. Ricart, J. Rubio, F. Illas and J. M. Jimenez-Mateos, J. Am. Chem. Soc. 118, 8071 (1996).
32 K. Suenaga, M. P. Johansson, N. Hellgren, E. Broitman, L. R. Wallenberg, C. Colliex, J. E. Sundgren and L. Hultman, Chem. Phys. Lett. 300, 695 (1999).
33 H. Sjőstrőm, C. Goze, P. Bernier and A. Rubio, Phys. Rev. Lett. 75, 1136 (1995).

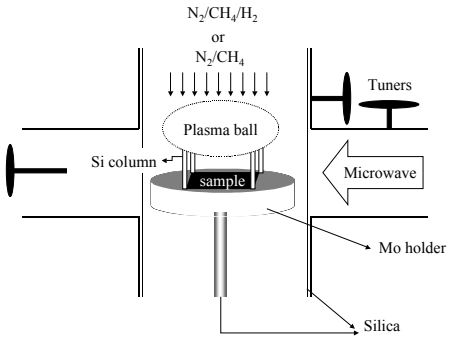

Fig. 1 Relative positions between Si columns and the sample in a reactor.

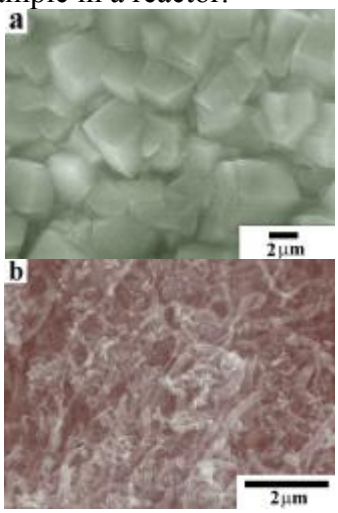

Fig. 2 SEM morphologies of (a) Si-C-N crystals, (b) Si-C-N nanotubes formed using Co catalyst film.

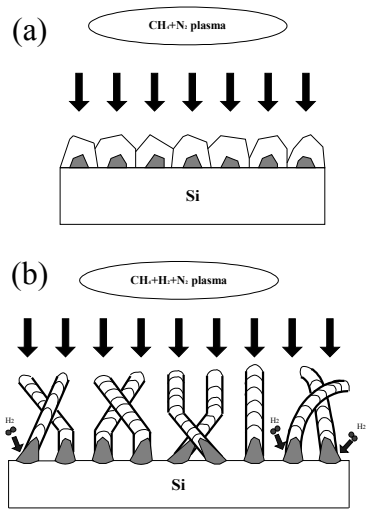

Fig. 3 Growth model of (a) Si-C-N crystals (b) Si-C-N nanotubes.

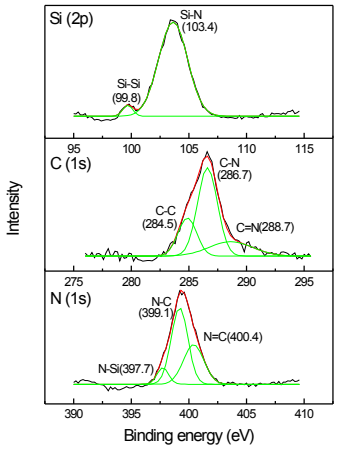

Fig. 4 XPS spectrum of Si-C-N crystals (a) Si (2p) core level, (b) C (1s) core level and (c) N (1s) core level.

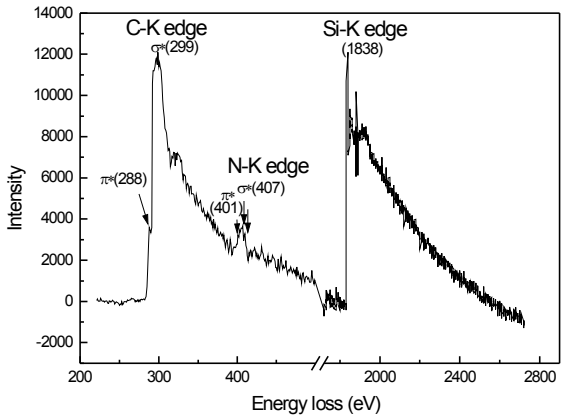

Fig. 5 EELS spectrum of Si-C-N nanotube recorded from the tube walls shown in Fig. 6 (b)

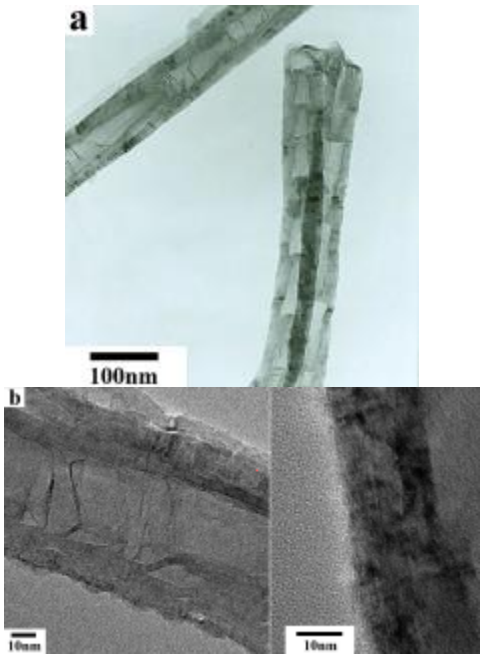

Fig. 6 TEM images of Si-C-N nanotube at (a) low magnification (b) high magnification.